

First-principles assessment of CO₂ capture mechanisms in aqueous piperazine (PZ)
solution

(Supporting Information)

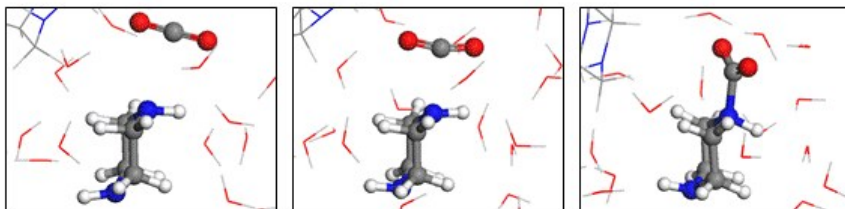
Haley M. Stowe,^a Eunsu Paek,^b and Gyeong S. Hwang^{a,b,}*

^aMaterials Science and Engineering Program and ^bMcKetta Department of Chemical
Engineering, University of Texas at Austin, Austin, Texas 78712, USA.

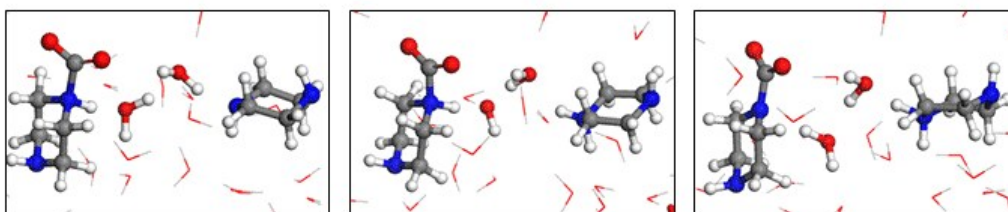
*Author to whom correspondence should be addressed:

Tel: 1-512-471-4847, Fax: 1-512-471-7060, E-mail: gshwang@che.utexas.edu

(a) $\text{PZ} + \text{CO}_2 \rightarrow \text{PZ}^+\text{COO}^-$ (CO_2 binding and zwitterion formation)



(b) $\text{PZH}^+\text{COO}^- + \text{H}_2\text{O} + \text{PZ} \rightarrow \text{PZCOO}^- + \text{PZH}^+ + \text{H}_2\text{O}$ (deprotonation by water)



(c) $\text{PZH}^+\text{COO}^- + \text{PZ} \rightarrow \text{PZCOO}^- + \text{PZH}^+$ (deprotonation by a nearby PZ)

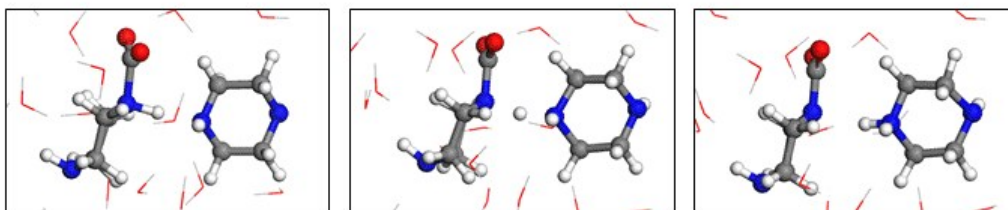


Figure S1. Observed elementary reaction mechanisms during CO_2 capture in aqueous piperazine from AIMD simulations at 400 K. System contains 2 PZ, 1 CO_2 and 20 H_2O molecules in cubic box with edge length 9.76 Å which represents approximately 30 wt% PZ. Zwitterion formation (a), followed by deprotonation to another PZ through the water network (b) or direct proton transfer (c). Red, gray, blue and white balls represent O, C, N and H atoms, respectively.

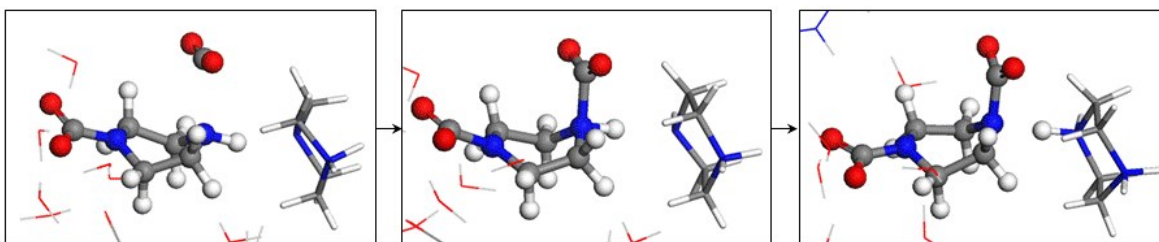


Figure S2. AIMD snapshots demonstrating CO_2 binding to PZCOO^- and subsequent deprotonation to form COO-PZCOO^- ($\text{PZCOO}^- + \text{CO}_2 + \text{H}^+ \rightarrow \text{COO-PZCOO}^- + \text{H}^+$) at 400 K. System contains 4 PZCOO^- , 4 PZH^+ , 4 CO_2 and 8 H_2O molecules in cubic box with edge length 12.066 Å.

Energy Cutoff Verification

Table S1. Total energy changes (ΔE in kcal/mol) during formation of H^+PZCOO^- shown in Fig. 6 [(a) \rightarrow (b), (a) \rightarrow (c), (a) \rightarrow (d)] with varying cutoff energies (350, 400, 450 and 500 eV).

Cutoff Energy (eV)	(a) \rightarrow (b)	(a) \rightarrow (c)	(a) \rightarrow (d)
350	-15.9	-6.7	-32.1
400	-16.5	-8.6	-31.2
450	-16.8	-9.0	-30.6
500	-16.9	-8.9	-30.4

Reaction Energetic Calculation Details Using Implicit Solvent Model

The changes in Gibbs free energy in the aqueous phase ΔG_{aq}° were calculated for the $\text{XH}^+ \rightarrow \text{H}^+ + \text{X}$ reactions (where X is PZ, PZH^+ , PZCOO^- or COO-PZCOO^-) to estimate the pKa values in Table 1 using the standard thermodynamic cycle shown below where the gaseous energy changes ($\Delta G_{gas}^{\circ}(react \rightarrow prod)$) were corrected for a difference in solvation energies ($\Delta \Delta G_{solv}^{\circ}(react \rightarrow prod)$).

$$\Delta G_{aq}^{\circ} = \Delta G_{gas}^{\circ}(react \rightarrow prod) + \Delta \Delta G_{solv}^{\circ}(react \rightarrow prod)$$

$$\Delta G_{aq}^{\circ} = \sum \Delta G_{gas}^{\circ}(products) - \sum \Delta G_{gas}^{\circ}(reactants) + \sum \Delta G_{solv}^{\circ}(products) - \sum \Delta G_{solv}^{\circ}(reactants)$$

The SMD model¹ within the polarizable continuum model (PCM) approach was used for implicit

solvation. The pKa can then be calculated via the following relation: $pK_a = \frac{\Delta G_{aq}^{\circ}}{RT \ln 10}$. All free energies were also corrected for the change in standard state going from gas phase (1 atm) to solution (1 mol/l) ($\Delta G_{gas}^* \rightarrow \Delta G_{gas}^{\circ}$) by adding a factor of 1.89 kcal/mol. Following the recommendations of many authors, instead of attempting to calculate the $\Delta G_{solv}^{\circ}(\text{H}^+)$, we use the recommended experimental values, which are known to give better quantitative estimates for the overall reaction energetics.¹ This approach was also used to calculate ΔH_{aq}° for the $2\text{PZ} + \text{CO}_2(\text{g}) \rightarrow \text{PZCOO}^- + \text{PZH}^+$ reaction; note that CO_2 in the gas phase was used as the reference in this case.

Table S2. Free energy change (in kcal/mol) for the $\text{XH}^+ \rightarrow \text{X} + \text{H}^+$ reactions [$\text{X} = \text{PZ}$, PZH^+ , PZCOO^- (both protonation at $\text{N}_{\text{PZCOO}^-}$ and O site considered), or COO-PZCOO^- (protonation at both N and O sites considered)] predicted from static QM calculations at a theory level of B3LYP/6-311++G(d,p) with SMD solvation model. Estimated and experimental pKa values also listed.

Species	ΔG_{solv}°	ΔG_{gas}°	$\Delta \Delta G_{solv}^{\circ}$	ΔG_{aq}°	pKa (calc)	pKa (exp)
PZ	-11.22	219.24	-206.18	13.06	9.58	9.73 ²
PZH ⁺	-69.65	113.46	-107.66	5.80	4.26	5.33 ²
H ⁺ PZH ⁺	-226.60					
PZCOO ⁻	-75.90	*	*	*	*	
H ⁺ PZCOO ⁻	-60.01	293.90	-280.49	13.41	9.83	9.15 ³ -9.44 ^{4,5}
PZCOOH	-15.22	336.33	-325.29	11.04	8.10	

COO-PZCOO ⁻	-191.12	392.76	-381.28	11.48	8.42
HOOC-PZCOO ⁻	-74.45				

*Protonation at N_{PZCOO⁻} site (H⁺PZCOO⁻) and at O site (PZCOOH) considered.

For comparison to ΔH calculated using AIMD simulations in Section 3.5, we also calculated ΔH for the $2\text{PZ} + \text{CO}_2(\text{g}) \rightarrow \text{PZH}^+ + \text{PZCOO}^-$ using an implicit solvent model. The predicted ΔH of -0.49 kcal/mol CO_2 from the static QM calculation is much smaller in magnitude than those from previous experiments and our AIMD simulations. This implies that the implicit solvent method may underestimate the solvation energies of charged products (PZH⁺ and PZCOO⁻) relative to PZ, as also discussed in earlier theoretical studies.⁶ We also estimated ΔG_{aq}° for the (i) PZH⁺ + PZCOO⁻ \rightarrow PZ + H⁺PZCOO⁻ and the (ii) PZCOO⁻ + H⁺PZCOO⁻ \rightarrow PZH⁺ + COO-PZCOO⁻ reactions using static QM calculations with implicit solvent for comparison to the ΔA values from AIMD simulations (Table 1), as shown in Table S3 below.

Table S3. Predicted enthalpy and free energy changes in kcal/mol using static QM calculations at a theory level of B3LYP/6-311++G(d,p). Entropy changes in cal/mol/K also included.

Reaction	ΔH_{gas}^0	ΔG_{gas}^0	$\Delta\Delta H_{solv}^0$	$\Delta\Delta G_{solv}^0$	ΔH_{aq}^0	ΔG_{aq}^0	ΔS_a
PZH ⁺ + PZCOO ⁻							
\rightarrow	-74.46	-74.66	74.33	74.34	-0.13	-0.32	0.64
PZ + H ⁺ PZCOO ⁻							
PZCOO ⁻ + H ⁺ PZCOO ⁻							
\rightarrow	125.12	125.56	-124.32	-124.89	0.81	0.68	0.44
PZH ⁺ + COO-PZCOO ⁻							

Here, ΔG_{aq}° for reaction (i) is predicted to be -0.32 kcal/mol, and ΔG_{aq}° for reaction (ii) is predicted to be 0.68 kcal/mol. Using this method, not only proton transfer between PZ/PZCOO⁻, but also COO-PZCOO⁻ relative to PZCOO⁻/H⁺PZCOO⁻ formation, appear to have similar thermodynamic favorability. This is likely related to the inadequacy of this method to describe the solvation structure and dynamics. As shown in Table S4 below, the entropies do not vary much between the gas phase and when using an implicit solvent. In addition, while the vibrational entropies of the individual species are similar as in AIMD simulations (shown in Table S6), the rotational and translational entropies are much higher in the implicit solvent case. This demonstrates that the translational and rotational entropies of the species may be significantly reduced in the solvent environment relative to the gas phase. This effect may not be adequately described if explicit solvent molecules are not included. Further, the implicit solvent method does not include the effects of the change in the entropy of the solvent molecules, which is likely to be a predominant factor in the sizeable ΔS values predicted from AIMD simulations.

Table S4. Predicted translational, rotational, vibrational, and total entropies (S) in cal/mol/K of each species in the gas phase and in implicit solvent using static QM calculations at B3LYP/6-311++G(d,p) level of theory.

	H ₂ O		PZ		PZH ⁺		PZCOO ⁻		H ⁺ PZCOO ⁻		COO ⁻ PZCOO ⁻	
	S _{gas}	S _{aq}	S _{gas}	S _{aq}	S _{gas}	S _{aq}	S _{gas}	S _{aq}	S _{gas}	S _{aq}	S _{gas}	S _{aq}
S _{translational}	34.61	34.61	39.27	39.27	39.31	39.31	40.48	40.48	40.50	40.50	41.34	41.34
S _{rotational}	11.85	10.49	26.15	26.16	26.26	26.25	28.83	28.84	28.89	28.89	30.78	30.78
S _{vibrational}	0.01	0.01	7.98	7.88	8.40	8.14	18.70	17.79	19.87	18.75	29.70	29.87
S	46.47	45.11	73.40	73.31	73.96	73.70	88.01	87.11	89.26	88.14	101.82	101.97

Predicted Entropies from AIMD Simulations

In order to test whether the sampling time is sufficient for the entropy calculations, the entropies were calculated using 10, 20, and 30 ps trajectories from one case for each system as shown in Table S5 below.

Table S5. Absolute entropies (cal/mol/K) from 10, 20, and 30 ps trajectories where each system contains 30 H₂O with PZ, PZH⁺, PZCOO⁻, H⁺PZCOO⁻ or COO⁻PZCOO⁻ molecules in a cubic periodic box with side length as indicated in Table S6.

	10 ps	20 ps	30 ps
PZ	423.48	413.75	407.16
PZH ⁺	385.35	393.21	394.62
PZCOO ⁻	429.23	425.50	427.54
H ⁺ PZCOO ⁻	399.69	412.66	410.55
COO ⁻ PZCOO ⁻	451.41	438.75	448.59

Table S6. Translational, rotational, vibrational, and total entropies (cal/mol/K) used in ΔE , ΔS , and ΔA calculations presented in Table 1 from AIMD simulations at 298 K. Each system contains 30 H₂O and 1 PZ, PZH⁺, PZCOO⁻, H⁺PZCOO⁻ or COO⁻PZCOO⁻ molecules in a cubic periodic box with side length as indicated in the table. The densities correspond to 1.01 g/cm³.

	H ₂ O	PZ	Total	H ₂ O	PZH ⁺	Total	H ₂ O	PZCOO ⁻	Total
S _{translational}	10.41	16.93	329.83	10.50	15.90	331.63	11.38	17.41	357.70
S _{rotational}	1.31	12.97	52.63	1.32	11.46	50.73	1.39	12.38	54.08
S _{vibrational}	0.03	7.68	8.84	0.03	8.48	9.75	0.03	17.45	18.27
S	11.75	37.58	391.30	11.85	35.84	392.11	12.80	47.24	430.05
Box Size (Å)	10.11			10.11			10.34		

	H ₂ O	H ⁺ PZCOO ⁻	Total	H ₂ O	COO ⁻ PZCOO ⁻	Total
S _{translational}	10.90	17.45	342.77	11.28	17.06	356.46
S _{rotational}	1.28	11.50	49.54	1.49	12.88	57.15
S _{vibrational}	0.03	17.97	18.84	0.03	27.57	28.38

S	12.21	46.93	411.16	12.79	57.51	441.99
Box Size (Å)	10.34			10.56		

To estimate how ΔA may change when the amine species are allowed to interact, we placed 57 H₂O molecules with 2 amine molecules (corresponding to approximately 15 wt% PZ) described as follows. For the PZH⁺ + PZCOO⁻ \leftrightarrow PZ + H⁺PZCOO⁻ reaction, the PZH⁺/PZCOO⁻ pair or the PZ/H⁺PZCOO⁻ pair was placed in a cubic periodic box with side length 12.57 Å. The density of this system corresponds to 1.04 g/cm³, respectively, which is reasonable with experimental values.⁷

Table S7. Total energy (E), entropy (S), and free energy (A) changes for the PZH⁺ + PZCOO⁻ \leftrightarrow PZ + H⁺PZCOO⁻ reaction at 298 K from AIMD simulations when amine pairs are placed in same simulation box with 57 H₂O molecules.

Reaction	ΔE (kcal/ mol CO ₂)	ΔS (cal/ mol CO ₂ /K)	ΔA (kcal/ mol CO ₂)
PZH ⁺ + PZCOO ⁻ \rightarrow PZ + H ⁺ PZCOO ⁻	-7.1	6.7	-9.1

Entropy Calculations from Classical MD Simulations

In addition to predicting entropy changes from molecular motion (translational, rotational, and vibrational) of each aqueous amine system, we also considered the change in configurational entropy due to the composition difference between the reactant (S_R) and product (S_P) systems in the classical MD simulations. The configurational entropy in cal/mol CO₂/K is given by $S_C = -Nk \sum x_i \ln x_i$ where N is the number of PZ per CO₂, k is the Boltzmann constant, and x_i is the fraction of PZ/PZH⁺/PZCOO⁻/H⁺PZCOO⁻/COO⁻PZCOO⁻ relative to the total amount of PZ. As shown in Tables S8 and S9 below, the inclusion of ΔS_c does not significantly change the entropic favorabilities presented in Tables 2 and 3.

Table S8. Predicted entropy changes from molecular motion (translational, rotational, and vibrational) ($\Delta S = S_P - S_R$ in cal/mol CO₂/K) and different compositions (configurational) (ΔS_c in cal/mol CO₂/K) from classical MD simulations at 298 K for the PZH⁺ + PZCOO⁻ → PZ + H⁺PZCOO⁻ reaction at varying PZ concentrations (wt%) and CO₂ loadings ($\alpha = \text{mol CO}_2/\text{mol PZ}$), as indicated. S_P and S_R compositions are shown in Table 2. Systems representing 15 (30) wt% PZ solution contains 1960 (1600) H₂O molecules.

	ΔS	ΔS_c	$\Delta S + \Delta S_c$
Case (i) 15 wt% ($\alpha=0.16$)	13.98	-5.08	8.90
Case (ii) 30 wt% ($\alpha=0.16$)	13.25	-4.97	8.28
Case (iii) 30 wt% ($\alpha=0.33$)	13.98	-2.75	11.23

Table S9. Predicted entropy changes from molecular motion (translational, rotational, and vibrational) ($\Delta S = S_P - S_R$ in cal/mol CO₂/K) and different compositions (configurational) (ΔS_c in cal/mol CO₂/K) from classical MD simulations at 298 K for the PZCOO⁻ + H⁺PZCOO⁻ → COO⁻PZCOO⁻ + PZH⁺ reaction at varying conversions (X). S_P and S_R compositions are shown in Table 3. All systems represent 30 wt% PZ solution at 0.67 CO₂ loading and contain 1600 H₂O molecules.

	ΔS	ΔS_c	$\Delta S + \Delta S_c$
Case (iv) ($X=20\%$)	-2.84	0.46	-2.38
Case (v) ($X=50\%$)	-6.84	0.43	-6.41
Case (vi) ($X=100\%$)	-9.92	-1.38	-11.30

We also calculated entropy changes using classical MD simulations for the systems used to predict the entropy changes from AIMD simulations where the amines are well-dispersed (presented in Table 1). The relative entropic favorabilities for the reactions are similar between the two simulation methods, as shown in Table S10 below. This suggests that the change in entropic favorabilities in the classical MD simulations where the amine species are allowed to interact (Tables 2 and 3) may be attributed to the aggregation of the amines when the amines are not well-dispersed, rather than due to the use of a classical force field.

Table S10. Predicted changes in the total entropy (ΔS in cal/mol CO₂/K) from AIMD and classical MD simulations at 298 K for the listed reactions in aqueous solution. Each PZ, PZCOO⁻, PZH⁺, H⁺PZCOO⁻ or COO⁻PZCOO⁻ was placed in a cubic periodic box with 30 H₂O molecules, corresponding to approximately 15 wt%; further details of simulation conditions can be found in Table S6.

Reaction	ΔS (Classical MD)	ΔS (AIMD)
PZH ⁺ + PZCOO ⁻ → PZ + H ⁺ PZCOO ⁻	-3.7	-19.7
PZCOO ⁻ + H ⁺ PZCOO ⁻ → PZH ⁺ + COO ⁻ PZCOO ⁻	-0.5	-3.7

Table S11. Translational, rotational and vibrational entropies (cal/mol/K) and total entropies (cal/mol CO₂/K) used in ΔS calculations presented in Table 2, from classical MD simulations at 298 K.

System Composition (Box Size in Å) [Density in g/cm ³]	1960 H ₂ O, 51 PZ, 12 PZH ⁺ , 12 PZCOO ⁻ (41.14) [1.01]					1960 H ₂ O, 63 PZ, 12 H ⁺ PZCOO ⁻ (41.21) [1.00]			
	H ₂ O	PZ	PZH ⁺	PZCOO ⁻	Total	H ₂ O	PZ	H ⁺ PZCOO ⁻	Total
S _{translational}	11.56	15.66	14.94	14.99	1981.97	11.59	15.76	15.50	1989.61
S _{rotational}	2.41	14.00	13.46	12.86	472.92	2.43	13.78	13.69	476.70
S _{vibrational}	0.00	8.03	7.80	17.16	59.08	0.00	8.31	18.04	61.64
S	13.97	37.69	36.20	45.01	2513.97	14.02	37.85	47.23	2527.95

System Composition (Box Size in Å) [Density in g/cm ³]	1600 H ₂ O, 100 PZ 25 PZH ⁺ , 25 PZCOO ⁻ (41.07) [1.03]					1600 H ₂ O, 125 PZ, 25 H ⁺ PZCOO ⁻ (41.17) [1.02]			
	H ₂ O	PZ	PZH ⁺	PZCOO ⁻	Total	H ₂ O	PZ	H ⁺ PZCOO ⁻	Total
S _{translational}	10.95	15.24	14.48	14.30	788.52	11.04	15.42	15.13	797.29
S _{rotational}	2.29	13.55	13.10	12.32	221.39	2.34	13.66	13.53	224.98

$S_{\text{vibrational}}$	0.00	8.50	7.48	17.00	58.40	0.00	8.29	17.88	59.29
S	13.24	37.29	35.06	43.62	1068.30	13.38	37.36	46.54	1081.56

System Composition (Box Size in Å) [Density in g/cm ³]	1600 H ₂ O, 50 PZ 50 PZH ⁺ , 50 PZCOO ⁻ (41.05) [1.06]					1600 H ₂ O, 100 PZ, 50 H ⁺ PZCOO ⁻ (41.25) [1.04]			
	H ₂ O	PZ	PZH ⁺	PZCOO ⁻	Total	H ₂ O	PZ	H ⁺ PZCOO ⁻	Total
$S_{\text{translational}}$	10.72	15.06	14.33	14.13	385.26	10.97	15.25	14.62	395.19
$S_{\text{rotational}}$	2.25	13.39	13.24	12.53	108.37	2.29	13.65	13.14	111.01
$S_{\text{vibrational}}$	0.00	8.46	7.65	17.13	33.15	0.00	8.41	17.79	34.57
S	12.97	36.91	35.21	43.79	526.79	13.26	37.31	45.55	540.77

System Composition (Box Size in Å) [Density in g/cm ³]	1600 H ₂ O, 50 PZH ⁺ , 50 PZCOO ⁻ , 50 H ⁺ PZCOO ⁻ (41.25) [1.09]				
	H ₂ O	PZH ⁺	PZCOO ⁻	H ⁺ PZCOO ⁻	Total
$S_{\text{translational}}$	10.75	14.05	14.22	14.37	192.56
$S_{\text{rotational}}$	2.23	12.81	12.36	12.96	53.47
$S_{\text{vibrational}}$	0.00	7.44	16.92	17.93	21.12
S	12.98	34.30	43.49	45.26	267.15

System Composition (Box Size in Å) [Density in g/cm ³]	1600 H ₂ O, 60 PZH ⁺ , 40 PZCOO ⁻ , 40 H ⁺ PZCOO ⁻ , 10 COO-PZCOO ⁻ (41.17) [1.10]					
	H ₂ O	PZH ⁺	PZCOO ⁻	H ⁺ PZCOO ⁻	COO-PZCOO ⁻	Total
$S_{\text{translational}}$	10.63	14.09	14.12	14.17	13.52	190.37
$S_{\text{rotational}}$	2.20	12.77	12.24	13.08	11.37	52.94
$S_{\text{vibrational}}$	0.00	7.75	17.13	17.57	25.25	21.00
S	12.82	34.61	43.49	44.82	50.14	264.31

System Composition (Box Size in Å) [Density in g/cm ³]	1600 H ₂ O, 75 PZH ⁺ , 25 PZCOO ⁻ , 25 H ⁺ PZCOO ⁻ , 25 COO-PZCOO ⁻ (41.08) [1.11]					
	H ₂ O	PZH ⁺	PZCOO ⁻	H ⁺ PZCOO ⁻	COO-PZCOO ⁻	Total
$S_{\text{translational}}$	10.51	13.74	13.72	14.21	12.95	187.78
$S_{\text{rotational}}$	2.15	12.64	12.37	12.83	10.97	51.76
$S_{\text{vibrational}}$	0.00	7.71	17.02	18.05	25.19	20.78

S	12.66	34.10	43.11	45.08	49.12	260.31
---	-------	-------	-------	-------	-------	--------

System Composition (Box Size in Å) [Density in g/cm ³]	1600 H ₂ O, 100 PZH ⁺ , 50 COO-PZCOO ⁻ (40.92) [1.12]			
	H ₂ O	PZH ⁺	COO-PZCOO ⁻	Total
S _{translational}	10.41	13.67	12.84	185.73
S _{rotational}	2.14	12.66	11.03	51.29
S _{vibrational}	0.00	7.74	25.20	20.21
S	12.54	34.07	49.08	257.23

Classical Force Fields Employed in This Work

The nonbonding ($E_{nonbond}$), bond (E_{bond}), angle (E_{angle}), and torsion ($E_{torsion}$) energies are summed to calculate the total energy (E_{total}). The nonbonding energy for each pair includes Coulomb interaction and van der Waals interaction in the 12-6 Lennard-Jones form. Bond and angle energies were expressed in the harmonic form. The dihedral and improper torsion energies were expressed according to the form used in the Amber force field⁸.

$$E_{total} = E_{bond} + E_{angle} + E_{torsion} + E_{nonbond}$$

$$E_{bond} = \sum_i k_{b,i} (r_i - r_{0,i})^2$$

$$E_{angle} = \sum_i k_{\theta,i} (\theta_i - \theta_{0,i})^2$$

$$E_{torsion} = \sum_i K [1 + \cos\left(\frac{n\phi - d}{\phi}\right)]$$

$$E_{nonbond} = \sum_i \sum_{j>i} \left[\frac{q_i q_j e^2}{r_{ij}} + 4\epsilon_{ij} \left[\left(\frac{\sigma_{ij}}{r_{ij}}\right)^{12} - \left(\frac{\sigma_{ij}}{r_{ij}}\right)^6 \right] \right]$$

Here, $k_{b,i}$, $k_{\theta,i}$, represent the bond and angle force constants, respectively. K is the torsion energy coefficient, n is the periodicity of the torsion, d is the phase offset, and ϕ is the dihedral angle. $r_{0,i}$ and $\theta_{0,i}$ are the bond distance and bond angle at equilibrium, respectively. For $E_{nonbond}$, q_i is the partial atomic charge, r_{ij} is the distance between atoms i and j , and ϵ_{ij} and σ_{ij} are the Lennard-Jones parameters which refers to the depth of the potential well and the distance where the potential is zero, respectively. A modified version of the EPM2 force field with flexible bonds and angles was used for CO₂.^{9,10} The partial atomic charges for PZ, PZCOO⁻, PZH⁺, H⁺PZCOO⁻, and COO⁻PZCOO⁻ were obtained from QM calculations at the B3LYP/6-311+G(d,p) level of theory and using the Merz-Singh-Kollman scheme.¹¹ The rest of the force field parameters were obtained from the general Amber force field.^{8,12} The Coulomb and L-J energies were calculated between atoms separated by three or more bonds. The 1-4 L-J and Coulomb energies were scaled by 1/2 and 5/6, respectively. The Lorentz-Berthelot combination rule was applied for unlike atom pairs where $\epsilon_{ij} = \sqrt{\epsilon_i \epsilon_j}$ and $\sigma_{ij} = (\sigma_i + \sigma_j)/2$.

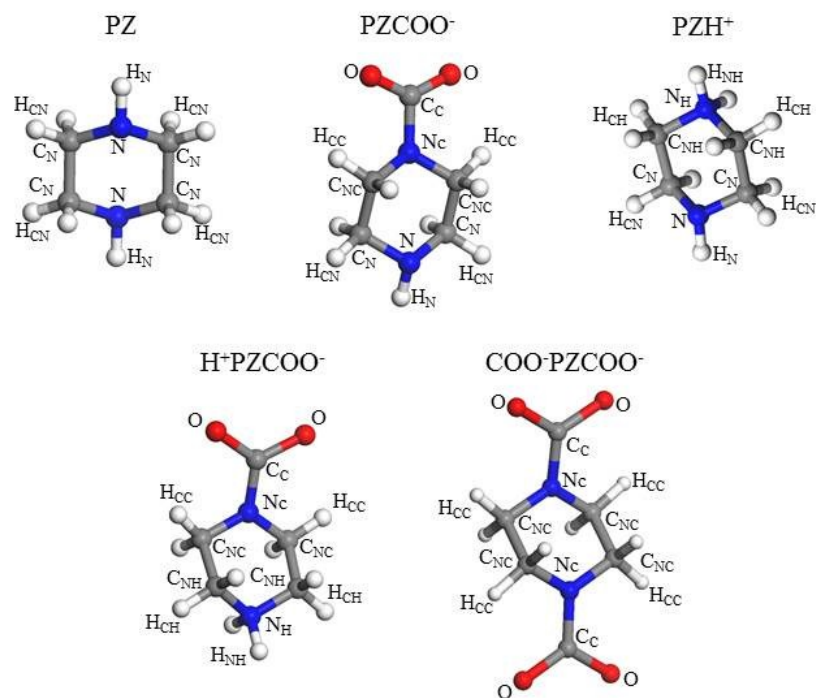


Figure S3. Structures of PZ, PZCOO⁻, PZH⁺, H⁺PZCOO⁻ and COO-PZCOO⁻ with corresponding atom types for force field parameters listed in Tables S12-S16.

Table S12. Nonbonded force field parameters

Species	Atom	q_i	σ_i (Å)	ϵ_i (kcal/mol)
PZ	N	-0.7004	3.340	0.1700
	C _N	0.0727	3.399	0.1094
	H _N	0.3566	1.069	0.0157
	H _{CN}	0.0496	2.650	0.0157
PZCOO ⁻	N _C	-0.2803	3.250	0.1700
	N	-0.7465	3.340	0.1700
	C _C	0.9024	3.399	0.0860
	O	-0.8111	2.960	0.2100
	H _N	0.3482	1.069	0.0157
	C _{NC}	-0.0075	3.399	0.1094
	C _N	0.0209	3.399	0.1094
	H _{CC} H _{CN}	0.0530 0.0399	2.650 2.650	0.0157 0.0157
PZH ⁺	N _H	-0.1931	3.340	0.1700
	N	-0.7311	3.340	0.1700
	H _{NH}	0.3182	1.069	0.0157
	H _N	0.4024	1.069	0.0157
	C _N	0.2931	3.399	0.1094
	C _{NH}	-0.3386	3.399	0.1094
	H _{CN} H _{CH}	0.0316 0.2125	2.650 2.650	0.0157 0.0157
	H ⁺ PZCOO ⁻	N _H	-0.2235	3.340
N _C		-0.4410	3.250	0.1700
C _{NC}		0.1530	3.399	0.1094
C _{NH}		-0.2195	3.399	0.1094
C _C		0.8711	3.399	0.0860
H _{NH} H _{CC} /H _{CH}		0.3054 0.0946	1.069 2.650	0.0157 0.0157
O		-0.7206	2.960	0.2100
COO ⁻ PZCOO ⁻		N _C	-0.2392	3.250
	C _{NC}	-0.1386	3.399	0.1094
	C _C	0.9762	3.399	0.0860
	O	-0.8785	2.960	0.2100
	H _{CC}	0.0743	2.650	0.0157
CO ₂	O	-0.3256	3.033	0.1600
	C	0.6512	2.757	0.0560

Table S13. Bond parameters

Species	Bond Type	k_b (kcal/mol/Å ²)	r_0 (Å)
PZ/PZCOO ⁻ /PZH ⁺ / H ⁺ PZCOO ⁻ /COO ⁻ PZCOO ⁻	C _N - C _{N/NC/NH}	303.1	1.535
	C _{N/NC/NH} - H _{CN/CC/CH}	337.0	1.092
PZ/PZCOO ⁻ /PZH ⁺	N - C _N	320.6	1.470
	N - H _N	394.1	1.018
PZCOO ⁻ /H ⁺ PZCOO ⁻ / COO ⁻ PZCOO ⁻	N _C - C _{NC}	330.6	1.460
	N _C - C _C	478.2	1.345
	C _C - O	648.0	1.214
PZH ⁺ /H ⁺ PZCOO ⁻	N _H - H _{NH}	369.0	1.033
	N _H - C _{NH}	293.6	1.499
CO ₂	C - O	1283.38	1.149

Table S14. Angle parameters

Species	Angle Type	k_θ (kcal/mol/rad ²)	θ_0 (°)
PZ/PZCOO ⁻ /PZH ⁺ / H ⁺ PZCOO ⁻ /COO ⁻ PZCOO ⁻	N _{/C/H} - C _{N/NC/NH} - H _{CN/CC/CH}	49.42	109.80
	C _{N/NC/NH} - C _{N/NC/NH} - H _{CN/CC/CH}	46.37	110.05
	H _{CN/CC/CH} - C _{N/NC/NH} - H _{CN/CC/CH}	39.43	108.35
PZ/PZCOO ⁻ /PZH ⁺	N - C _N - C _{N/NC/NH}	66.18	110.38
	C _N - N - C _N	64.01	110.90
	C _N - N - H _N	47.13	109.92
PZCOO ⁻ /H ⁺ PZCOO ⁻ / COO ⁻ PZCOO ⁻	N _C - C _{NC} - C _N	65.85	112.13
	C _{NC} - N _C - C _{NC}	63.13	115.56
	O - C _C - O	78.17	130.38
	O - C _C - N _C	75.83	122.03
	C _C - N _C - C _{NC}	63.42	121.35
PZH ⁺ /H ⁺ PZCOO ⁻	H _{NH} - N _H - H _{NH}	40.52	108.11
	C _{NH} - N _H - H _{NH}	46.19	110.11
	N _H - C _{NH} - H _{CH}	49.01	107.90
	C _{NH} - N _H - C _{NH}	62.84	110.64
	N _H - C _{NH} - C _N	64.45	114.32
CO ₂	O - C - O	56.53	180

Table S15. Dihedral torsion parameters

Species	Dihedral Type	K (kcal/mol)	n	d (°)
PZ/PZCOO ⁻ /PZH ⁺ / H ⁺ PZCOO ⁻ /COO ⁻ PZCOO ⁻	X - C _N - C _{N/NC/NH} - X	0.156	3	0
PZ/PZCOO ⁻ /PZH ⁺	X - N - C _N - X	0.300	3	0
PZCOO ⁻ /H ⁺ PZCOO ⁻ / COO ⁻ PZCOO ⁻	C _N - C _{NC} - N _C - C X - N _C - C - X	0.530 2.500	1 2	0 180
PZH ⁺ /H ⁺ PZCOO ⁻	X - C _{NH} - N _H - X	1.400	3	0

Table S16. Improper torsion parameters

Species	Dihedral Type	K (kcal/mol)	n	d (°)
PZCOO ⁻ /H ⁺ PZCOO ⁻ / COO ⁻ PZCOO ⁻	N - C _N - O - O	10.5	2	180

References

- [1] A. V Marenich, C. J. Cramer and D. G. Truhlar, *J. Phys. Chem. B*, 2009, **113**, 6378–6396.
- [2] H. B. Hetzer, R. A. Robinson and R. G. Bates, *J. Phys. Chem.*, 1968, **72**, 2081–2086.
- [3] S. Bishnoi and G. T. Rochelle, *Chem. Eng. Sci.*, 2000, **55**, 5531–5543.
- [4] V. Ermatchkov, Á. Pérez-Salado Kamps and G. Maurer, *J. Chem. Thermodyn.*, 2003, **35**, 1277–1289.
- [5] P. W. J. Derks, T. Kleingeld, C. van Aken, J. A. Hogendoorn and G. F. Versteeg, *Chem. Eng. Sci.*, 2006, **61**, 6837–6854.
- [6] G. S. Hwang, H. M. Stowe, E. Paek and D. Manogaran, *Phys. Chem. Chem. Phys.*, 2015, **17**, 831–839.
- [7] S. A. Freeman and G. T. Rochelle, *J. Chem. Eng. Data*, 2011, **56**, 574–581.
- [8] W. D. Cornell, P. Cieplak, C. I. Bayly, I. R. Gould, K. M. Merz, D. M. Ferguson, D. C. Spellmeyer, T. Fox, J. W. Caldwell and P. A. Kollman, *J. Am. Chem. Soc.*, 1995, **117**, 5179–5197.
- [9] J. G. Harris and K. H. Yung, *J. Phys. Chem.*, 1995, **99**, 12021–12024.
- [10] S.-N. Huang, T. A. Pascal, W. A. Goddard, P. K. Maiti and S.-T. Lin, *J. Chem. Theory Comput.*, 2011, **7**, 1893–1901.
- [11] U. C. Singh and P. A. Kollman, *J. Comput. Chem.*, 1984, **5**, 129–145.
- [12] J. Wang, R. M. Wolf, J. W. Caldwell, P. A. Kollman and D. A. Case, *J. Comput. Chem.*, 2004, **25**, 1157–74.